A Variational Multiscale Method for Poisson's Equation in Mixed Form

Mats G. Larson[†], Axel Målqvist[‡], and Robert Söderlund[§]

Abstract

In this paper we present the adaptive variational multiscale method for solving the Poisson equation in mixed form. We use the method introduced in [3], and further analyzed and applied to mixed problems in [4], which is a general tool for solving linear partial differential equations with multiscale features in the coefficients. We extend the numerics in [4] from rectangular meshes to triangular meshes which allow for computation on more complicated domains. A new a posteriori error estimate is also included, which is used in an adaptive algorithm. We present a numerical example that shows the efficiency of incorporating a posteriori based adaptivity into the method.

1 Introduction

Multiscale problems appear in many applications in engineering and sciences, for instance, composite materials, flow in porous media, fluid mechanics, and quantum physics. A common feature of multiscale problems is that they are very computationally challenging and often impossible to solve to an acceptable tolerance with standard methods using only one mesh. Thus multiscale methods are introduced, which uses both local and global information computed on different scales.

[†] Professor of Applied Mathematics, Department of Mathematics, Umeå University, SE-901-87 Umeå, Sweden, mats.larson@math.umu.se.

[‡] Assistant Professor, Department of Information Technology, Uppsala University, SE-751-05 Uppsala, Sweden, axel.malqvist@it.uu.se.

[§] Research Assistant, Department of Mathematics, Umeå University, SE-901-87 Umeå, Sweden, robert.soderlund@math.umu.se.

Multiscale methods have been developed in various ways the last 15 years. A common feature is that information from decoupled local fine scale equations are used to modify the coarse scale solution. Two early examples are the multiscale finite element method [1] and the variational multiscale method [2]. The adaptive variational multiscale method was first introduced by Larson and Målqvist in [3], which presents a posteriori error estimates that can be used in adaptive algorithms. That method is extended to mixed problems in [4], and further developed in e.g [5].

This paper is based on [4], but we extend the numerics to triangular meshes which allows for more complicated geometries. We also derive a new improved a posteriori error estimate. This error estimate is used in an adaptive algorithm, that automatically tunes the parameters of the method.

2 Preliminaries

We let $\Omega \subset \mathbf{R}^d$ be a domain with Lipschitz boundary $\partial\Omega$. We consider a coarse scale and a fine scale, both of which need to be discretized. We denote the coarse mesh by $\mathcal{K}_H$, with H_K we refer to the diameter of the elements in the coarse mesh, and we let $H = \max_K H_K$. The coarse mesh satisfies $\cup_{K\in\mathcal{K}_H} K = \Omega$ where all K are disjoint. The fine mesh however, is only defined on local subregions $\omega \subset \Omega$, since we wish to decouple the fine scale computations. The meshes will be nested so that all of those subregions are made up of coarse elements. We therefore introduce the following notation, $\mathcal{K}_H(\omega) = \{K \in \mathcal{K}_H : K \in \omega\}$ and with $\mathcal{K}_h(\omega)$ we refer to the set of fine scale elements $\{K\}$ such that $\cup_{K\in\mathcal{K}_h(\omega)} K = \omega$. Since the meshes are nested all $K \in \mathcal{K}_H(\omega)$ can be written as a union of elements in $\mathcal{K}_h(\omega)$. The diameter of the elements $K \in \mathcal{K}_h(\Omega)$ will be denoted h_K, and we let $h = max_K h_K$.

Next we define the function spaces $\mathcal{V} = \{\boldsymbol{v} \in H(div;\Omega) : \boldsymbol{n}\cdot\boldsymbol{v} = 0 \text{ on } \partial\Omega\}$ and $\mathcal{W} = L^2(\Omega)$, where $\boldsymbol{n}$ is the outward unit normal to $\partial\Omega$. The corresponding finite element spaces on the coarse scale will be denoted $\mathcal{V}_c$ and $\mathcal{W}_c$ respectively, and we let

$$\mathcal{V}_c = \mathcal{RT}_H, \tag{1a}$$

$$\mathcal{W}_c = \mathcal{P}_H, \tag{1b}$$

where $\mathcal{P}_H$ is the space of piecewise constants on the coarse mesh, and $\mathcal{RT}_H$ is the space of lowest order Raviart-Thomas elements on the coarse mesh. We want an hierarchical split between the coarse and the fine scales and if we introduce the operators $\Pi_H : \mathcal{V} \to \mathcal{V}_c$ and $P_H : \mathcal{W} \to \mathcal{W}_c$, as the Raviart-Thomas interpolant and L^2-projection onto the coarse scale spaces respectively, we can define the fine scale spaces $\mathcal{V}_f$, $\mathcal{W}_f$ by

$$\mathcal{V}_f = \{\boldsymbol{v} \in \mathcal{V} : \Pi_H \boldsymbol{v} = \boldsymbol{0}\}, \tag{2a}$$
$$\mathcal{W}_f = \{v \in \mathcal{W} : P_H v = 0\}. \tag{2b}$$

We let $\mathcal{P}_h(\omega)$ and $\mathcal{RT}_h(\omega)$ be the piecewise constants, and the lowest order Raviart-Thomas elements, on the subgrid $\mathcal{K}_h(\omega)$. The fine scale finite element spaces can now be defined in the following way

$$\mathcal{P}_h^f(\omega) = \{v \in \mathcal{P}_h(\omega) : P_H v = 0\}, \tag{3a}$$
$$\mathcal{RT}_h^f(\omega) = \{\boldsymbol{v} \in \mathcal{RT}_h(\omega) : \Pi_H \boldsymbol{v} = \boldsymbol{0} \text{ and } \boldsymbol{n} \cdot \boldsymbol{v} = 0 \text{ on } \partial\omega\}, \tag{3b}$$

where, $\mathcal{P}_h^f(\omega)$ approximates $\mathcal{W}_f$ and $\mathcal{RT}_h^f(\omega)$ approximates $\mathcal{V}_f$ on the subregion ω.

The patches ω_i on which we define the fine scale finite element spaces, are defined in the following way.

Definition 2.1. *We say that ω_i^1 is a 1-layer patch if $\omega_i^1 = supp(\boldsymbol{\phi}_i)$, where $\boldsymbol{\phi}_i$ is a coarse Raviart-Thomas basis function. Further we say that ω_i^n is an n-layer patch if,*

$$\omega_i^n = \cup_{\{i: supp(\theta_i) \cap \omega_i^{n-1} \neq \emptyset\}} supp(\theta_i), \quad n = 2, 3, \ldots \tag{4}$$

where θ_i is a coarse scale continous piecewise linear nodal basis function. In the text we omit the superscript n.

Let us also introduce the fine scale projection operator $P_{h,\omega} : \mathcal{W} \to \mathcal{P}_h^f(\omega)$ and the Scott-Zhang interpolants $P_H^1 : \mathcal{V} \to \mathcal{P}_H^1$ and $P_{h,\omega,0}^1 : \mathcal{V} \to \mathcal{P}_{h,0}^1$, where the latter projects onto functions that are zero on the boundary.

3 A Variational Multiscale Decomposition of Poisson's Equation in Mixed Form

The equation we wish to solve is the Poisson equation in mixed form, which reads: find the pressure $u \in \mathcal{W}$ and the flux $\boldsymbol{\sigma} \in \mathcal{V}$ such that

$$\tfrac{1}{a}\boldsymbol{\sigma} = \nabla u, \qquad \text{in } \Omega, \tag{5a}$$
$$-\nabla \cdot \boldsymbol{\sigma} = f, \qquad \text{in } \Omega, \tag{5b}$$
$$n \cdot \boldsymbol{\sigma} = 0, \qquad \text{on } \partial\Omega, \tag{5c}$$

where $a \in L^\infty(\Omega)$ is the permeability satisfying $a \geq a_0 > 0$ for some constant a_0, and $f \in L^2(\Omega)$ is a given external force such that $\int_\Omega f dx = 0$. We use the variational multiscale framework, see [2], and let $u = u_c + u_f$, $\boldsymbol{\sigma} = \boldsymbol{\sigma}_c + \boldsymbol{\sigma}_f$, where $\boldsymbol{\sigma}_c \in \mathcal{V}_c$, $u \in \mathcal{W}_c$, $\boldsymbol{\sigma}_f \in \mathcal{V}_f$, and $u_f \in \mathcal{W}_f$. Let φ_k denote the piecewise constant basis functions on the coarse mesh, such that $\mathcal{W}_c = span(\{\varphi_k\}_{\mathcal{M}})$, where $\mathcal{M}$ is the set of coarse scale elements. Also let $\mathcal{N}$ be the set of coarse faces and ψ_i be the partition of unity defined by $\psi_i = \frac{1}{d+1}$ on $supp(\boldsymbol{\phi}_i)$ ($\boldsymbol{\phi}_i$ being the continuous piecewise linear nodal basis functions). As in [4], the multiscale finite element solution $\boldsymbol{\Sigma}$ corresponding to $\boldsymbol{\sigma}$, is given by $\boldsymbol{\Sigma} = \sum_{i\in\mathcal{N}} \Sigma_c^i(\boldsymbol{\phi}_i + \boldsymbol{\xi}_i) + \boldsymbol{\beta}$, where $\boldsymbol{\beta} = \sum_{i\in\mathcal{N}} \boldsymbol{\beta}_i$, and

$$(\tfrac{1}{a}\sum_{j\in\mathcal{N}} \Sigma_c^j \boldsymbol{\phi}_j, \boldsymbol{\phi}_i) + (\tfrac{1}{a}\sum_{j\in\mathcal{N}} \Sigma_c^j \boldsymbol{\xi}_j, \boldsymbol{\phi}_i) - (\sum_{k\in\mathcal{M}} U_c^k \varphi_k, \nabla\cdot\boldsymbol{\phi}_i) = -(\tfrac{1}{a}\boldsymbol{\beta}, \boldsymbol{\phi}_i), \tag{6a}$$

$$(\nabla\cdot\sum_{j\in\mathcal{N}} \Sigma_c^j \boldsymbol{\phi}_j, \varphi_k) = -(f, \varphi_k), \tag{6b}$$

$$\forall i\in\mathcal{N}, \forall k\in\mathcal{M},$$

$$\begin{aligned}
(\tfrac{1}{a}\boldsymbol{\xi}_i, \boldsymbol{v}_f) + (\eta_i, \nabla\cdot\boldsymbol{v}_f) &= -(\tfrac{1}{a}\boldsymbol{\phi}_i, \boldsymbol{v}_f), && \forall \boldsymbol{v}_f \in \mathcal{RT}_h^f(\omega_i), \forall i\in\mathcal{N}, && (7a)\\
-(\nabla\cdot\boldsymbol{\xi}_i, w_f) &= 0, && \forall w_f \in \mathcal{P}_h^f(\omega_i), \forall i\in\mathcal{N}, && (7b)
\end{aligned}$$

$$\begin{aligned}
(\tfrac{1}{a}\boldsymbol{\beta}_i, \boldsymbol{v}_f) + (\rho_i, \nabla\cdot\boldsymbol{v}_f) &= 0, && \forall \boldsymbol{v}_f \in \mathcal{RT}_h^f(\omega_i), \forall i\in\mathcal{N}, && (8a)\\
-(\nabla\cdot\boldsymbol{\beta}_i, w_f) &= (f, \psi_i w_f), && \forall w_f \in \mathcal{P}_h^f(\omega_i), \forall i\in\mathcal{N}. && (8b)
\end{aligned}$$

4 A Posteriori Error Estimate

In this section we present an a posteriori error estimate for the proposed multiscale method. For simplicity we assume two spatial dimensions and that a is piecewise constant. We follow ideas presented in [6], page 26-29. We start by presenting a technical Lemma.

Lemma 4.1. *Let $\mathcal{P}_h^1(\omega) \subset H^1(\omega)$ be the space of continuous piecewise linear functions and let $\mathcal{RT}_h(\omega)$ be the space of lowest order Raviart-Thomas finite elements on a given triangulation $\mathcal{K}$ of a domain $\omega \subset \Omega$. Further let $\nabla\times\phi = [\partial\phi/\partial y, -\partial\phi/\partial x]$, for any $\phi \in H^1(\omega)$. Then*

(i) $\nabla\times\phi_h \in \mathcal{RT}_h$ for all $\phi_h \in \mathcal{P}_h^1(\omega)$.
(ii) For any function ϕ_h that vanishes on the boundary $\partial\omega$ we have that $\boldsymbol{n}\cdot\nabla\times\phi_h = 0$ on the boundary $\partial\omega$, $\boldsymbol{n}$ being the normal of the boundary $\partial\omega$.

Proof. For (i) we refer to [6] and (ii) is easily seen since if ϕ_h vanishes on the boundary, the gradient $\nabla\phi_h = [\partial\phi_h/\partial x, \partial\phi_h/\partial y]$ must be parallell to $\boldsymbol{n}$ and thus the curl $\nabla\times\phi_h = [\partial\phi_h/\partial y, -\partial\phi_h/\partial x]$ must be orthogonal to $\boldsymbol{n}$.

We are now ready to present the main theorem.

Theorem 4.1. *We let* $\boldsymbol{\Sigma} = \sum_{i\in\mathcal{N}} \Sigma_c^i(\boldsymbol{\phi}_i + \boldsymbol{\xi}_i) + \boldsymbol{\beta}$ *be the multiscale approximation of* $\boldsymbol{\sigma}$ *and assume* $d = 2$. *It holds,*

$$\|\frac{1}{\sqrt{a}}(\boldsymbol{\sigma} - \boldsymbol{\Sigma})\|^2_{L^2(\Omega)} \leq C \sum_{i\in\mathcal{N}} \sum_{K\in\mathcal{K}(\omega_i)} h_K^2 \|f\psi_i + \nabla\cdot(\Sigma_c^i(\boldsymbol{\phi}_i + \boldsymbol{\xi}_i) + \boldsymbol{\beta}_i)\|^2_{L^2(K)} \tag{9}$$

$$+ \sum_{i\in\mathcal{N}} \sum_{K\in\mathcal{K}_h(\omega_i)} h_K \|[\boldsymbol{t}\cdot\frac{1}{a}(\Sigma_c^i(\boldsymbol{\phi}_i + \boldsymbol{\xi}_i) + \boldsymbol{\beta}_i)]\|^2_{L^2(\partial K)}$$

$$+ \sum_{i\in\mathcal{N}} H\|\tilde{\Sigma}^i\|^2_{L^2(\partial\omega_i)}$$

where $[\cdot]$ *denotes the jump across the boundary* ∂K, $\boldsymbol{t}$ *is the tangent vector to* ∂K, *and* $\tilde{\Sigma}^i \in \mathcal{P}_h^1(\partial\omega_i)$ *is defined for each* $i \in \mathcal{N}$ *as the solution to,*

$$(\tilde{\Sigma}^i, v)_{L^2(\partial\omega_i)} = (\frac{1}{a}(\Sigma_c^i(\boldsymbol{\phi}_i + \boldsymbol{\xi}_i) + \boldsymbol{\beta}_i), \nabla\times v)_{L^2(\omega_i)}, \qquad \text{for all } v \in \mathcal{P}_h^1(\omega_i). \tag{10}$$

Proof. We note that there exists functions $\phi \in H^1(\Omega)$ and $\gamma \in H_0^1(\Omega)$ such that, $\boldsymbol{v} = a\nabla\gamma + \nabla\times\phi$ for all $\boldsymbol{v} \in (L^2(\Omega))^2$ and furthermore

$$\|\nabla\gamma\|_{L^2(\Omega)} + \|\nabla\phi\|_{L^2(\Omega)} \leq C\|\boldsymbol{v}\|_{L^2(\Omega)}. \tag{11}$$

We let $\boldsymbol{\sigma} - \boldsymbol{\Sigma} = a\nabla\gamma + \nabla\times\phi$ and get,

$$\|\frac{1}{\sqrt{a}}(\boldsymbol{\sigma} - \boldsymbol{\Sigma})\|^2_{L^2(\Omega)} = (\boldsymbol{\sigma} - \boldsymbol{\Sigma}, \nabla\gamma) + (\frac{1}{a}(\boldsymbol{\sigma} - \boldsymbol{\Sigma}), \nabla\times\phi) = \mathrm{I} + \mathrm{II}. \tag{12}$$

We treat the two terms separately.

We start with the first term and use Green's formula and the orthogonality given by the multiscale method, as well as interpolation estimates and equation (11), with a modified constant C depending on a.

$$\mathrm{I} = (\boldsymbol{\sigma} - \boldsymbol{\Sigma}, \nabla\gamma) = (-\nabla\cdot(\boldsymbol{\sigma} - \boldsymbol{\Sigma}), \gamma) \tag{13}$$

$$= (f + \nabla\cdot\boldsymbol{\Sigma}, \gamma - P_H\gamma) \tag{14}$$

$$= \sum_{i\in\mathcal{N}} (f\psi_i + \nabla\cdot(\Sigma_c^i(\boldsymbol{\phi}_i + \boldsymbol{\xi}_i) + \boldsymbol{\beta}_i), \gamma - P_H\gamma - P_{h,\omega_i}\gamma) \tag{15}$$

$$\leq C\left(\sum_{i\in\mathcal{N}} \sum_{K\in\mathcal{K}_h(\omega_i)} h_K^2 \|f\psi_i + \nabla\cdot(\Sigma_c^i(\boldsymbol{\phi}_i + \boldsymbol{\xi}_i) + \boldsymbol{\beta}_i)\|^2_{L^2(K)}\right)^{1/2} \tag{16}$$

$$\|\frac{1}{\sqrt{a}}(\boldsymbol{\sigma} - \boldsymbol{\Sigma})\|_{L^2(\Omega)},$$

Next we turn to the second term. We note that P^1 is the Scott-Zhang interpolant onto continuous piecewise linear functions and use Lemma 4.1 to subtract the curl of a continuous piecewise linear function,

$$\begin{aligned}
\mathrm{II} &= (\frac{1}{a}(\boldsymbol{\sigma} - \boldsymbol{\Sigma}), \nabla \times \phi) = -(\frac{1}{a}\boldsymbol{\Sigma}, \nabla \times \phi) && (17)\\
&= -(\frac{1}{a}\boldsymbol{\Sigma}, \nabla \times (\phi - P^1_H \phi)) && (18)\\
&= -\sum_{i\in\mathcal{N}} (\frac{1}{a}(\Sigma^i_c(\boldsymbol{\phi}_i + \boldsymbol{\xi}_i) + \boldsymbol{\beta}_i), \nabla \times (\phi - P^1_H \phi)) && (19)\\
&= -\sum_{i\in\mathcal{N}} (\frac{1}{a}(\Sigma^i_c(\boldsymbol{\phi}_i + \boldsymbol{\xi}_i) + \boldsymbol{\beta}_i), \nabla \times (I - P^1_{h,\omega_i})(\phi - P^1_H \phi)) && (20)\\
&\quad - \sum_{i\in\mathcal{N}} (\frac{1}{a}(\Sigma^i_c(\boldsymbol{\phi}_i + \boldsymbol{\xi}_i) + \boldsymbol{\beta}_i), \nabla \times (P^1_{h,\omega_i} - P^1_{h,\omega_i,0})(\phi - P^1_H \phi)),
\end{aligned}$$

where I is the identity operator. At this point we use Green's formula for the curl operator, that a is piecewise constant on the mesh and $\partial v_2/\partial x - \partial v_1/\partial y = 0$ for all $\boldsymbol{v} = [v_1, v_2] \in \mathcal{RT}_h(\omega)$ (since v_1 independent of y and v_2 independent of x for first order Raviart Thomas functions), and equation (10) to get,

$$\begin{aligned}
\mathrm{II} \leq C \sum_{i\in\mathcal{N}} \sum_{K\in\mathcal{K}_h(\omega_i)} &\|[\boldsymbol{t} \cdot \frac{1}{a}(\Sigma^i_c(\boldsymbol{\phi}_i + \boldsymbol{\xi}_i) + \boldsymbol{\beta}_i)]\|_{L^2(\partial K)} && (21)\\
&\cdot \|(I - P^1_{h,\omega_i})(\phi - P^1_H \phi)\|_{L^2(\partial K)}\\
+ C \sum_{i\in\mathcal{N}} &\|\tilde{\Sigma}^i\|_{L^2(\partial\omega_i)} \|P^1_{h,\omega_i}(\phi - P^1_H \phi)\|_{L^2(\partial\omega_i)}.
\end{aligned}$$

We use a trace inequality, that P^1 is stable in H^1, and the Scott-Zhang interpolation estimate (see [7]), to obtain

$$\begin{aligned}
\mathrm{II} \leq & C \sum_{i\in\mathcal{N}} \sum_{K\in\mathcal{K}_h(\omega_i)} h_K \|[\boldsymbol{t} \cdot \frac{1}{a}(\Sigma^i_c(\boldsymbol{\phi}_i + \boldsymbol{\xi}_i) + \boldsymbol{\beta}_i)]\|_{L^2(\partial K)} \|\nabla\phi\|_{L^2(K)} && (22)\\
& + C \sum_{i\in\mathcal{N}} H^{1/2} \|\tilde{\Sigma}^i\|_{L^2(\partial\omega_i)} \|\nabla\phi\|_{L^2(\omega_i)}\\
\leq & C \left(\sum_{i\in\mathcal{N}} \sum_{K\in\mathcal{K}_h(\omega_i)} h_K \|[\boldsymbol{t} \cdot \frac{1}{a}(\Sigma^i_c(\boldsymbol{\phi}_i + \boldsymbol{\xi}_i) + \boldsymbol{\beta}_i)]\|^2_{L^2(\partial K)} \right)^{1/2} && (23)\\
& \cdot \|\frac{1}{\sqrt{a}}(\boldsymbol{\sigma} - \boldsymbol{\Sigma})\|_{L^2(\Omega)}\\
& + C \left(\sum_{i\in\mathcal{N}} H \|\tilde{\Sigma}^i\|^2_{L^2(\partial\omega_i)} \right)^{1/2} \|\frac{1}{\sqrt{a}}(\boldsymbol{\sigma} - \boldsymbol{\Sigma})\|_{L^2(\Omega)}.
\end{aligned}$$

The theorem follows immediately.

We can now present an adaptive algorithm (Algorithm 1).

Algorithm 1

1: Start with the original mesh partition with 1-layer patches and zero level of refinements everywhere.
2: Compute $\boldsymbol{\Sigma}$.
3: Compute the terms in the right hand side of (9) and set

$$\begin{aligned} \eta_{r,i} &= \sum_{K \in \mathcal{K}_h(\omega_i)} h_K^2 \| f\psi_i + \nabla \cdot (\Sigma_c^i(\boldsymbol{\phi}_i + \boldsymbol{\xi}_i) + \boldsymbol{\beta}_i) \|^2_{L^2(K)} \\ &\quad + \sum_{K \in \mathcal{K}_h(\omega_i)} h_K \| [\boldsymbol{t} \cdot \frac{1}{a}(\Sigma_c^i(\boldsymbol{\phi}_i + \boldsymbol{\xi}_i) + \boldsymbol{\beta}_i)] \|^2_{L^2(\partial K)} \end{aligned} \tag{24a}$$

$$\eta_{l,i} = H \| \tilde{\Sigma}^i \|^2_{L^2(\partial \omega_i)} \tag{24b}$$

4: Modify the mesh according to the following:
- Increase the level of refinements on patch i if $\eta_{r,i} \geq \alpha_r max_i \eta_{r,i}$.
- Increase the number of layers on patch i if $\eta_{l,i} \geq \alpha_l max_i \eta_{l,i}$.

5: Stop when $\| \frac{1}{\sqrt{a}}(\boldsymbol{\sigma} - \boldsymbol{\Sigma}) \|^2_{L^2(\Omega)} / \| \frac{1}{\sqrt{a}} \boldsymbol{\sigma} \|^2_{L^2(\Omega)} \leq \mathrm{TOL}$, where TOL is a given tolerance.

5 Numerical example

In the numerical example we consider the domain $\Omega = [0,1] \times [0,1]$ and as our coarse mesh we use a Delaunay triangulation of Ω with $H \leq 0.1$. The fine scale mesh is obtained after two regular refinements of the coarse mesh.

We let $f = 1$ on the two fine scale elements in the lower left corner, $f = -1$ on the two fine scale elements in the upper right corner, and $f = 0$ everywhere else. Thus our problem can be seen as modeling an oil reservoir with injector at the lower left corner and producer at the upper right corner of the domain.

For the permeability a, we use a permeability from the tenth comparative SPE project. See Figure 2 for illustration of the permeability we use.

We use the adaptive algorithm 1 and study the convergence of $\boldsymbol{\Sigma}$. As a reference solution for $\boldsymbol{\sigma}$ we use a multiscale solution computed on a mesh with three level of refinements and four layers on all patches. We use $\alpha_r = \alpha_l = 0.1$ and TOL $= 0.05$. The convergence plot is found in Figure 1, with relative error plotted against average number of degrees of freedoms in the patches. We see that in average about 160 degrees of freedoms in the patches are required to reach the desired tolerance. A uniformly refined mesh with two levels of refinement and two layers for all patches only yielded a relative error of 0.068 with 371 degrees of freedom in average, i.e the adaptive procedure yields a far more efficient mesh than a uniformly refined mesh. Considering that relatively few iterations are needed to reach the desired tolerance the adaptive procedure is also time efficient. The resulting adaptively refined mesh is found in Figure 2. It is apparent and somewhat expected that it is important to refine close to the inlet and outlet. It is also clearly seen that the refinement follows the flow, i.e where the permeability is large.

References

1. Y. R. Efendiev, T. Y. Hou, and X. H. Wu, *Convergence of a nonconforming multiscale finite element method*, SIAM J. Num. Anal., 37, (2000), 888–910.
2. T. J. R. Hughes, *Multiscale phenomena: Green's functions, the Dirichlet-to-Neumann formulation, subgrid scale models, bubbles and the origins of stabilized methods,* Comput. Methods Appl. Mech. Engrg. 127, (1995), 387-401.
3. M. G. Larson and A. Målqvist, *Adaptive variational multiscale methods based on a posteriori error estimation: Energy norm estimates for elliptic problems,* Comput. Methods Appl. Mech. Engrg. 196, (2007), 2313-2324.
4. M. G. Larson and A. Målqvist, *A mixed adaptive variational multiscale method with applications in oil reservoir simulation,* Math. Models Methods Appl. Sci. 19, (2009), 1017-1042.
5. M. G. Larson and A. Målqvist, *Adaptive variational multiscale method of convection-diffusion problems*, Comm. Num. Methods Engrg. 25, (2009), 65-79,
6. D. Boffi, F. Brezzi, L. F. Demkowicz, R. G. Durán, R. S. Falk and M. Fortin, *Mixed finite elements, compatibility conditions, and applications* Springer Verlag, (2006)
7. L. R. Scott and S. Zhang, *Finite element interpolation of nonsmooth functions satisfying boundary conditions* Math. Comp, Vol. 54, No. 190, (1990), 483-493.

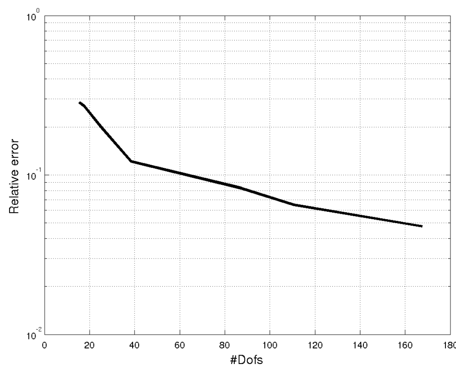

Fig. 1: The relative error approaching the desired tolerance in the adaptive algorithm.

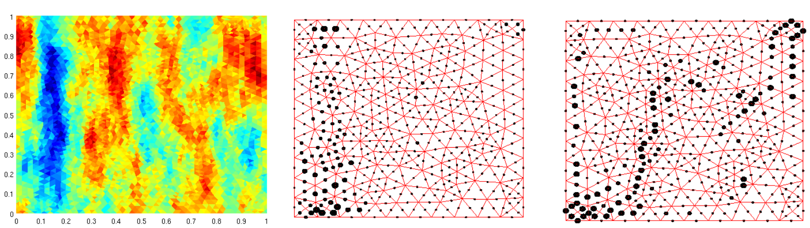

Fig. 2: The permeability function in log-scale and the adapted mesh. The thickness of the discs indicate the number of layers (in the middle) and number of refinements (to the right).